Al-Azhar University Civil Engineering Research Magazine (CERM)
Vol. (39) No. (4) October, 2017

EFFECTIVE WIDTH FOR THE INNER STIRRUPS HANGER STEEL OF LEDGE BEAM

Prof. Dr. Ayman Hussein[1], Dr. Mohamed Nabil[2], Dr. Ezz El-Deen Mostafa[2] and Eng. Yasser EL Sayed EL Badawy[3]

Structural Engineering Department, Faculty of Engineering, Ain Shams University, Cairo, Egypt

1. *Professor of R.C. structures*
2. *Ass. Professor, Structural Engineering Department*
3. *Structural Engineer*, Engineering for the Petroleum and Process Industries *Engineering Department*

ملخص البحث

تعتبر الكمرات الخرسانيه على شكل "L" ذات اهميه خاصه و تستخدم عادة ككمرات حاملة للمنشآت الخرسانية سابقة الصب . وتصمم هذه الكمرات طبقا للكود الأمريكي حيث يفترض أن الأفرع الخارجية للكانات الرأسية هي التي تقاوم الاجهادات الناتجة عن عزوم الالتواء وكذلك تعمل هذه الأفرع الخارجية للكانات كشداد لحمل الجزء السفلي من الكمرة . وعاده فأن عمل الأفرع الداخلية للكانات الرأسية كشداد يتم إهمالها في التصميم لذلك فإن الأفرع الخارجية للكانات تكون ذات أقطار كبيرة بالنسبة للأفرع الداخلية .

هذا البحث يعتمد البرنامج النظري الذي اعد خصيصا ويعتمد على دراسة مقدار مساهمة الأفرع الداخلية للكانات في العمل كشداد لحمل الجزء السفلي من الكمرة و كذلك حساب العرض الفعال لها .تم عمل دراسه ل 36 كمره باستخدام برنامج الحاسب الالي ABAQUS لدراسه تأثير تغيير ابعاد القطاع علي تحديد العرض الفعال للكانات الداخليه.

تم تصميم هذه الكمرات بحيث نضمن ان انهيار الجزء السفلي من الكمرة"Ledge" يحدث قبل انهيار الكمرة بالانحناء أو القص .

ABSTRACT

Ledge beams are commonly used as spandrels in precast concrete structures. The design of ledge beams according to the ACI code [1] and PCI [9] assumes that the outer branches of vertical stirrups are resisting torsion stress and acting as a hanger for the ledge part. The contribution of the inner vertical branches of stirrups as a hanger for the ledge part is neglected. Therefore, the outer vertical stirrups have a great amount of reinforcement with respect to the internal stirrups.

This paper presents the numerical study for the contribution of the internal vertical stirrups on the hanging action of the ledge and propose an equation for the estimating its effective width. The numerical analysis program using "ABAQUS" consists of modeling of 36 simply supported RC ledge beams with effective span 2700 mm to study the effect of changing ledge beam dimensions on the evaluating of the effective width for inner stirrups.

All beams were designed to ensure that the ultimate failure load of the ledge part due to yielding of the vertical hanger outer stirrups according to the ACI code [1] and PCI [9] was smaller than the ultimate flexural and punching shear failure loads of the specimens.

Key Words: Inner stirrups, Shear reinforcement, Ledge beam & Reinforced concrete.

1. INTRODUCTION

The design of ledge RC beams, commonly used as spandrels in precast concrete structures, may not be adequate under currently accepted criteria based on the ACI code [1] and the PCI Design Handbook [9]. That is because the actual behavior between the ledge part and the web part of the beam must be investigated. The current design procedure recommended by PCI Design Handbook [9] and ACI code [1] assumes that the outer branches of vertical stirrups are resisting torsion stress and acting as a hanger for the ledge. The contribution of the internal vertical branches of stirrups as a hanger for the ledge is neglected which is questionable. Therefore, the outer vertical stirrups have a great amount of reinforcement with respect to the internal stirrups. Also, the punching shear behavior of the ledge part must be considered to understand the load transfer from the ledge to the beam web. The failure of ledge part has many reasons such as bearing failure under loading plates, shear friction failure, flexural failure and punching failure.

The scope of this paper can be summarized as follow:

a) Studying numerically the effect of inner stirrups distribution on the hanging behavior of ledge part.

b) Evaluating the effective width of the inner stirrups hanger steel reinforcement of ledge beam.

2. FINITE ELEMENT MODEL

ABAQUS 6.10 are used to simulate the ledge beams. Geometry, loading and boundary conditions was modelled, as shown in Figure 1. The coordinate axes X, Y and Z are represented as axes 1, 2 and 3 in the model, respectively.

Also, the figure shows boundary conditions with restrained degrees of freedom with respect to each axe.

Regarding the FE models introduced in this research, three-dimensional 8-node reduced integration continuum elements (C3D8R - Bricks) are used to model the concrete beams. These elements are versatile and can be used in models for simple linear analysis or for complex nonlinear analyses involving contact, plasticity and relative horizontal displacement. Steel reinforcement bars are modelled using truss elements.

The accuracy of the results mainly relies on the FE mesh, constitutive material models and the boundary conditions. Therefore, these aspects are accurately investigated in the proposed FE model. There are several types of brick elements available in ABAQUS. For the analysis, (C3D8R) elements have been chosen with a maximum mesh size of 25 mm. The mesh intensity is the same for the whole concrete part of the model, as shown in Figure 2.

A regular structured hexahedral mesh is used, as shown in Figure 2.

Discrete reinforcement bars were defined using three-dimensional truss elements in linear order (T3D2). The former are used for all reinforcement types with a maximum mesh size of 25 mm. Moreover, Figure 3 shows internal steel reinforcement bars used in the models.

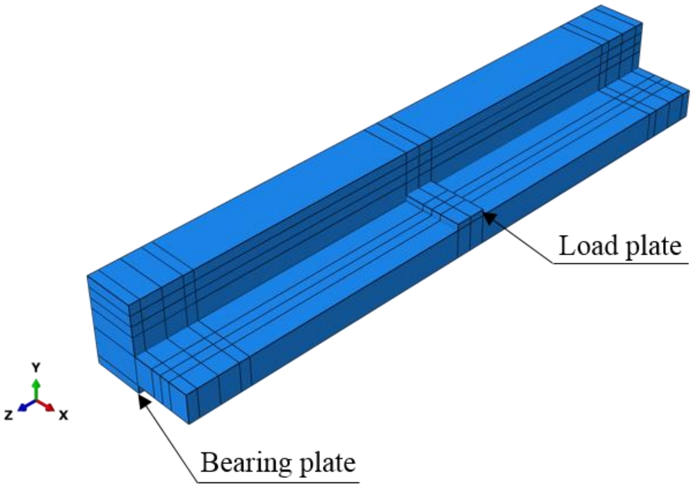

Figure (1): model of ledge beam.

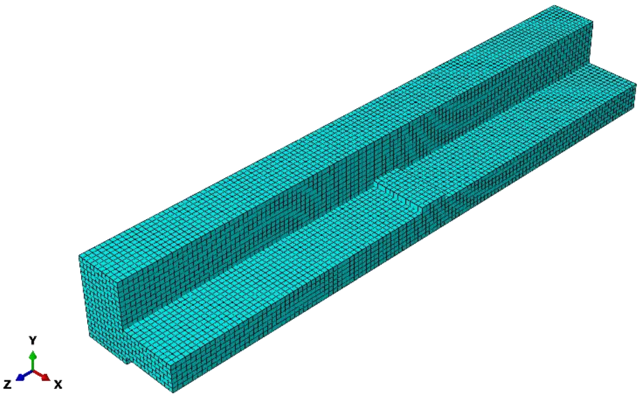

Figure (2): Finite element mesh of ledge beam.

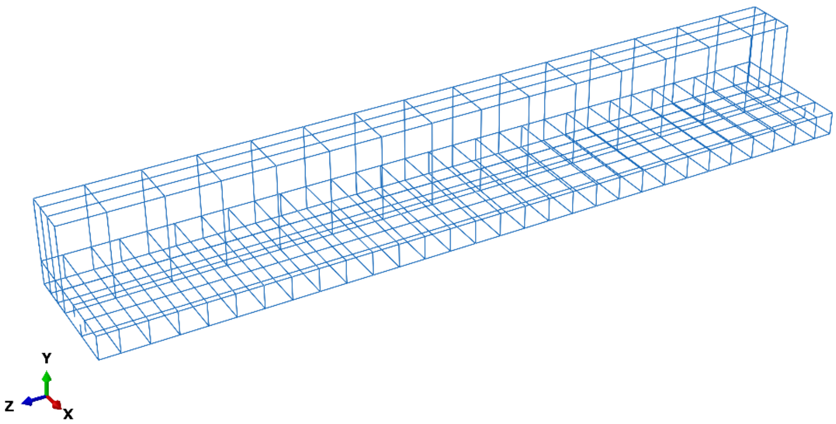

Figure (3): Internal steel reinforcement bars used in models

2.1. Material model

2.1.1 Concrete Modeling

ABAQUS 6.10 provides more than one model for the concrete. Concrete damage plasticity model is used to model the concrete ledge beam in the present study.

In this concrete damage plasticity model, all required input values related to concrete damage plasticity model are determined. The concrete dilation angle is taken as 45 for all beams. In addition, the other required parameters, namely, eccentricity, ratio of biaxial and uniaxial state strengths (fb_0/fc_0), ratio of the distance between the hydrostatic axis and deviatoric cross section (K), and viscosity parameter are taken as recommended in the ABAQUS manual (2010). Figure 4 shows the elastic–plastic behavior of concrete in compression is modeled according using Mander unconfined stress-strain curve which consists of a curved portion and a linear portion. The stress strain curve shown only the curved portion, concrete is modeled with Young`s modulus of 15.3 GPa.

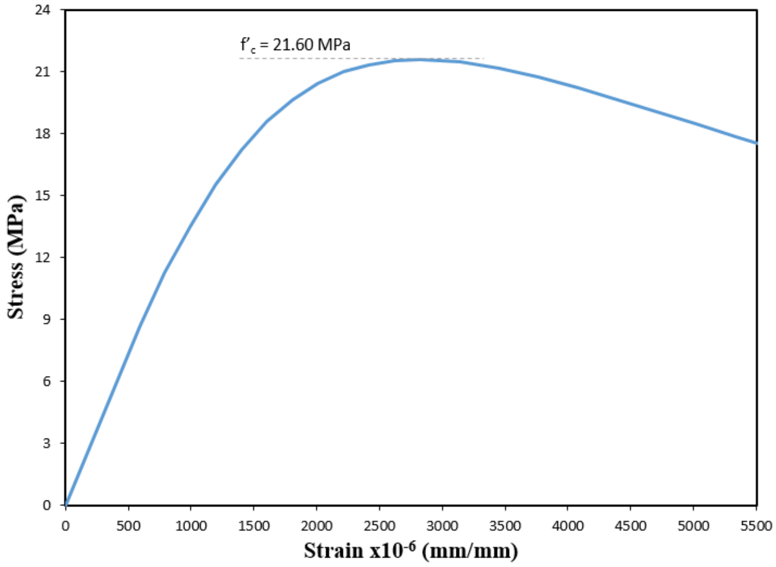

Figure (4): Uniaxial compressive stress-strain behavior of ledge beam.

2.1.2 Steel Reinforcement Modeling

The elastic properties of the steel reinforcement were 200 GPa for Young‟s modulus and 0.3 for the Poisson‟s ratio. Other mechanical properties, such as the yield stress and the ultimate strength are shown in Figure 5 Similar bilinear stress-strain relationship was adopted for the internal steel reinforcement material, as shown in Figure 5.

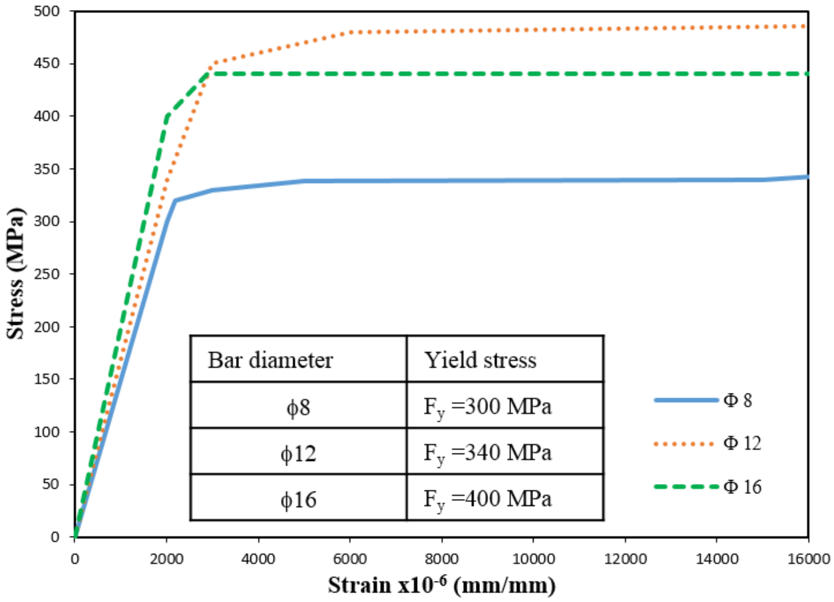

Figure (5): Bilinear stress-strain curve for steel.

2.2. Loading and boundary conditions

2.2.1 Applied Loads

The loading was applied as one concentrated load at the middle of the beam, as shown in Fig. 6 illustrates the load application for the beams.

The load was applied at the loading area as a concentrated load of 2.5 kN. The maximum number of increments was adjusted equal to 300 increments in all models. The static riks procedure involving the arc length method was used as an attempt to obtain the post-peak behavior. The geometric non-linearity was taken into consideration in the analysis in order to consider the second order effects. The Newton-Raphson iteration technique was used to get equilibrium at each load increment level.

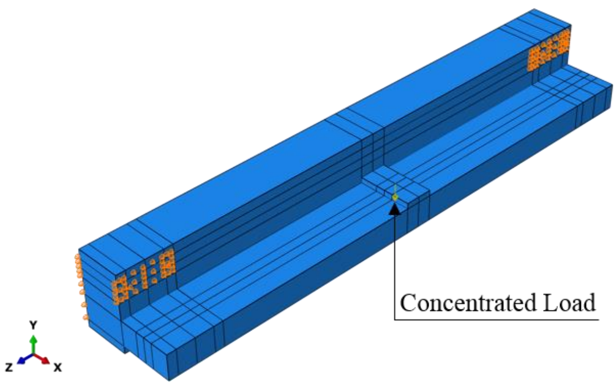

Figure (6): Concentrated load point of application.

2.2.2 supports modeling

Figure 7 and 8 illustrates the restraints adjusted in the FEA for the support condition. The two bottom bearing plates under the ledge beam were restrained from the translation in y-direction to simulate the hinged base provided by the bottom steel base used in the experimental program.

Moreover, all nodes on the front and back of the ledge beam with the same dimension of experimental steel plates were restrained from the translation in the x-direction to restrain the torsional moment. In addition, that all nodes where the anchors bolts tied the front and back steel plates were restrained from the translation in z-direction.

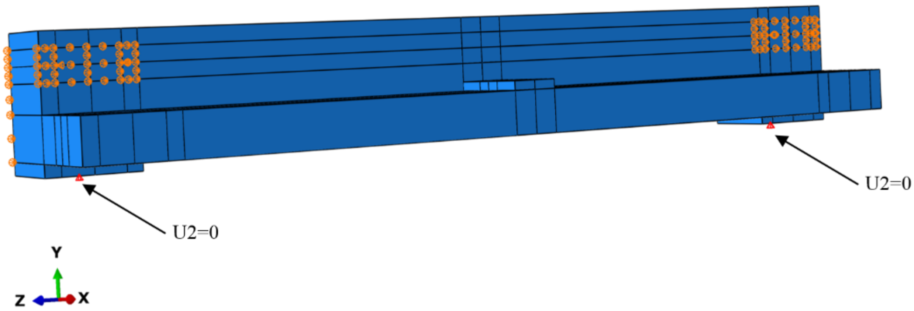

Figure (7): Vertical restraints of ledge beam.

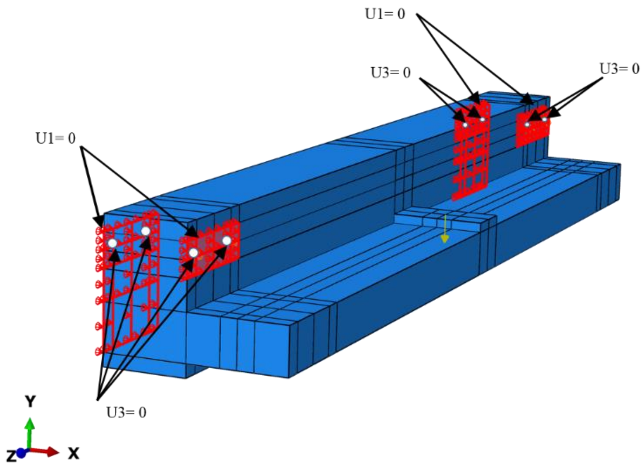

Figure (8): Horizontal restraints of ledge beam.

3. PARAMETRIC STUDY

In order to study the overall behavior of the inner stirrups hanger and estimates its effective width in ledge beams, a finite element method using ABAQUS 6.10 program is conducted on a total of 36 beams with the commonly variables in the ledge beam as the ledge depth and the web width, as shown in Tables 1 ,2 and 3. Each table shows a group of beams that has the same ledge depth. Fig.9 shows a schematic of the ledge beams, which are formed of ledge part depth = 140 mm, 160 mm and 180 mm. Web width of ledge beams = 250 mm, 300 mm and 350 mm are used with each ledge depth. In addition, all ledge beams are modeled as simply supported beams over clear spans of 2700 mm. All beams are subjected to one concentrated loads at mid of the beam span.

The main reason for changing the web width and the ledge depth of the ledge beam is to examine the predicted effective beam width with respect to the inner stirrups contribution at different beam dimension. The web stirrups consisted of external closed stirrups of rebar of 8 mm diameter with 200 mm spacing. The ledge part reinforcement consisted of closed stirrups of rebar of 12 mm diameter with 100 mm spacing. The top longitudinal reinforcement of the web, intermediate and bottom longitudinal reinforcement of the ledge part consisted of Rebar of 12 mm diameter. The bottom longitudinal reinforcement of the web consisted of rebar of 16 mm diameter. The stirrups are tied well to both top and bottom longitudinal steel reinforcement.

The inner stirrups for the web part of 8 mm diameter with 200 mm with three different values are adopted for the spacing between inner and outer stirrups S_i = 40 mm, 70 mm, or 100 mm to provide different levels of contribution between outer stirrups and inner stirrups.

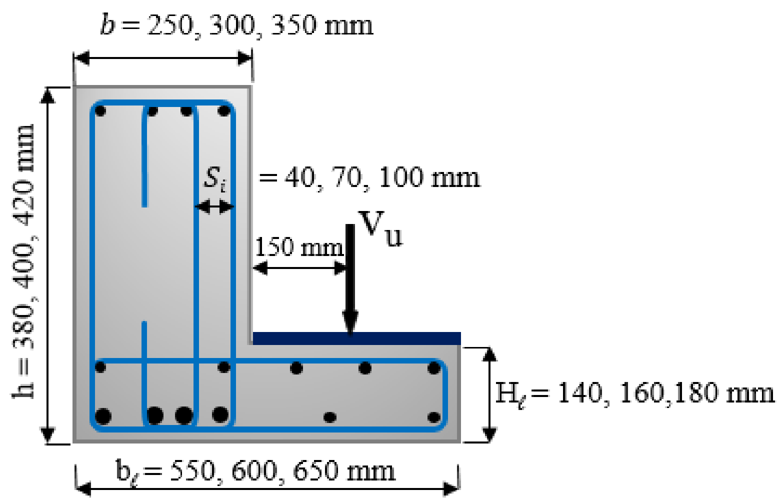

Figure (9): details of the used variables of the parametric study.

Table (1): Details of tested ledge beams with ledge depth 140 mm

Beam ID	b (mm) Web width	B_l (mm) Ledge width	h (mm) Beam depth	S_i (mm)
A1	250	550	380	Control Beam
A2				40
A3				70
A4				100
K1	300	600	380	Control Beam
K2				40
K3				70
K4				100
D1	350	650	380	Control Beam
D2				40
D3				70
D4				100

Table (2): Details of tested ledge beams with ledge depth 160 mm

Beam ID	b (mm) Web width	B_l (mm) Ledge width	h (mm) Beam depth	S_i (mm)
F1	250	550	400	Control Beam
F2				40
F3				70
F4				100
M1	300	600	400	Control Beam
M2				40
M3				70
M4				100
H1	350	650	400	Control Beam
H2				40
H3				70
H4				100

Table (3): Details of tested ledge beams with ledge depth 180 mm

Beam ID	b (mm) Web width	B_l (mm) Ledge width	h (mm) Beam depth	S_i (mm)
G1	250	550	420	Control Beam
G2				40
G3				70
G4				100
E1	300	600	420	Control Beam
E2				40
E3				70
E4				100
J1	350	650	420	Control Beam
J2				40
J3				70
J4				100

3.1. Results of parametric study

The obtained results of all the ledge beam models examined in the current parametric study are described and analyzed. This section illustrates the effect of using the inner stirrups on the behavior of ledge beams. In addition, this section presents a new proposed equation for calculating the inner stirrups effective width in terms of (S_i) which is the distance between the outer and inner stirrups.

A summary of ledge beams results, including the hanger failure load, punching failure load, mid-span deflection value at ultimate load and effective width for inner stirrups obtained from the numerical analysis models are presented in Tables 4, 5 and 6. It can be noted that each table shows the results of a certain group of beams that have the same ledge part thickness. Moreover, Tables 4, 5and 6 show the effective width factor (B_{ei}) obtained from the numerical analysis results at the hanger failure load by subsisting in Eq. (1) as follows:

$$\left[(w_b + B_{ei}\, h_l\,) * \frac{A_{sh(inner)} f_{y(inner)} \mathrm{d}_{s(inner)}}{m_d * S}\right] = [V_{uT} - V_{uC}] \qquad \text{Eq (1)}$$

Where;

V_{uT} = hanger failure load for the ledge beam with inner stirrups

V_{uC} = hanger failure load for the control ledge beam (without inner stirrups)

$A_{sh(inner)}$ = inner stirrups hanger steel area.

$f_{y(inner)}$ = yield strength of inner stirrups hanger reinforcement.

$d_{s(inner)}$ = distance measured from inner stirrups to the outer web side.

w_b = bearing plate width.

S = spacing between stirrups.

m_d $= \left[(d) - \left(3 - \frac{2h_l}{h}\right)\left(\frac{h_l}{h}\right)^2\left(\frac{b_l}{2}\right) - e\gamma_t \frac{(x^2y)_l}{\sum x^2y}\right]$

Tables 7 shows the ratios between the hanger capacities for the control beams (without inner stirrups) calculated according to PCI design handbook equation to the hanger capacities obtained from the FE program.

Table 7 shows that the hanger failure load calculated by PCI Design Handbook for the most of ledge beams are compatible with the FEA results which indicate a good agreement with the PCI design equation of the hanger steel reinforcement, in addition. It can be noticed that the hanger load capacity calculated by PCI increases with increasing the (bl/b) or (hl/h) ratios . Moreover, Table 7 shows that the ratios between PCI hanger load and FEA hanger load of the control ledge beam ranged from 0.90 to 1.14 depending on the available ledge beams dimensions (i.e. the web width, ledge depth, load eccentricity,…etc.) Numerical analysis is, however, required to further validate this ratio.

Figure 10 demonstrates the relationship between the ratio (hl/h) and the ratio between PCI hanger load and FEA hanger load of each control ledge beam. This relationship is plotted at three different ratios of (bl/b) = 1.85, 2.00 and 2.20. It can be noticed that PCI equation overestimated the hanger capacity for G1 by 14 % where the ratio (bl/b) = 2.20 and the ratio (hl/h) = 0.43 and underestimated the hanger capacity for H1 and D1 by 10% and 11% respectively where the ratio (bl/b) = 1.85 and the ratio (hl/h) = 0.40 and 0.36 respectively.

Table (4): Results of ledge beams with ledge depth 140 mm

Beam ID	b (mm) Web width	Hanger failure load (kN)	Punching failure load (kN)	$\square_m$ (mm)	B_{ei}	S_i (mm)
A1	250	124	204	40	N-A	Control Beam
A2		140	225	38	1.05	40
A3		132	223	40	0.195	70
A4		127	219	39	-0.48	100
K1	300	132	210	41	N-A	Control Beam
K2		146	235	39	0.69	40
K3		139	232	37	-0.06	70
K4		135	220	32	-0.56	100
D1	350	139	216	38	N-A	Control Beam
D2		153	244	36	0.61	40
D3		146	240	37	-0.13	70
D4		142	237	39	-0.61	100

Table (5): Results of ledge beams with ledge depth 160 mm

Beam ID	b (mm) Web width	Hanger failure load (kN)	Punching failure load (kN)	□$_m$ (mm)	B_{ei}	Si (mm)
F1	250	143	220	29	N-A	Control Beam
F2		158	250	40	0.65	40
F3		152	244	36	0.20	70
F4		147	241	38	-0.31	100
M1	300	153	231	34	N-A	Control Beam
M2		172	252	32	1.00	40
M3		164	250	33	0.35	70
M4		159	248	32	-0.11	100
H1	350	166	240	35	N-A	Control Beam
H2		184	255	26	0.84	40
H3		176	258	30	0.16	70
H4		170	255	31	-0.43	100

Table (6): Results of ledge beams with ledge depth 180 mm

Beam ID	b (mm) Web width	Hanger failure load (kN)	punching failure load (kN)	□$_m$ (mm)	B_{ei}	Si (mm)
G1	250	158	256	43	N-A	Control Beam
G2		178	273	42	0.88	40
G3		170	273	42	0.39	70
G4		167	270	42	0.31	100
E1	300	173	266	43	N-A	Control Beam
E2		190	272	29	0.60	40
E3		181	272	30	-0.06	70
E4		177	281	40	-0.38	100
J1	350	187	267	42	N-A	Control Beam
J2		214	282	27	1.39	40
J3		203	290	37	0.64	70
J4		197	289	39	0.21	100

Table (7): Numerical analysis hanger failure loads versus the PCI design handbook for the control beams

Beam ID	b_l / b	h_l / h	Hanger failure load (kN) FEA	Hanger failure load (kN) PCI	PCI / FEA
G1	2.20	0.43	158	181	1.14
F1		0.40	143	148	1.03
A1		0.36	124	120	0.97
E1	2.00	0.43	173	178	1.03
M1		0.40	153	148	0.97
K1		0.36	132	121	0.92
J1	1.85	0.43	187	177	0.94
H1		0.40	166	149	0.90
D1		0.36	139	124	0.89

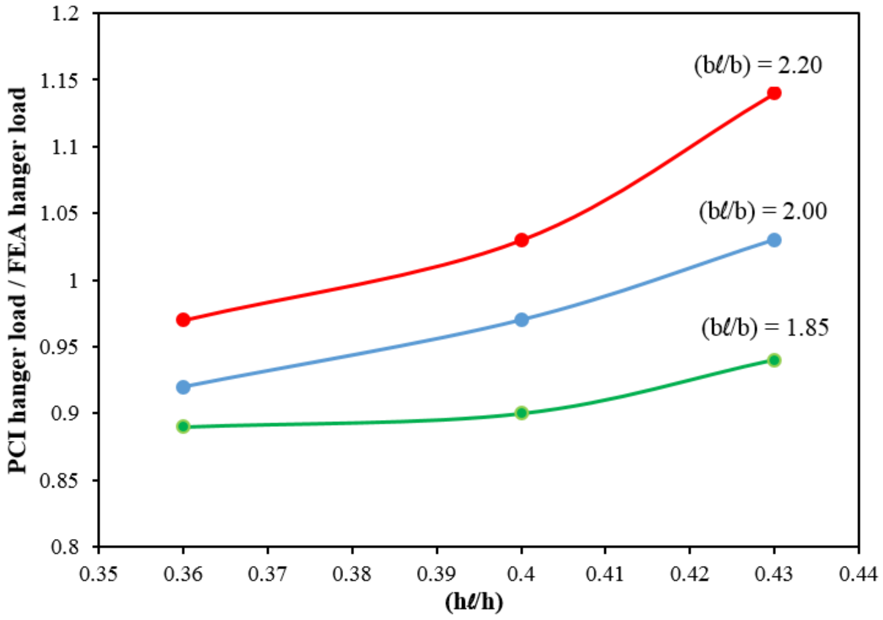

Figure (10): Effect of (bl/b) & (hl/h) ratios on ledge beams hanger capacity.

The values shown in tables 4, 5 and 6 were used to find a relationship between the distance S_i and the effective width factor (B_{ei}). Second-degree polynomial equation [Eq. (2)] was used to fit the calculated data.

$$B_{ei} = 1.50 * 10^{-4} * S_i^2 - 4.40 * 10^{-2} * S_i + 2.40 \quad \text{Eq.2}$$

Figure 11 shows the relation between the distance between the outer and inner stirrups (S_i) and the effective width factor (B_{ei}) in terms of the web widths 250 mm, 300 mm and 350 mm and the depths of ledge part 140 mm, 160 mm and 180 mm, respectively.

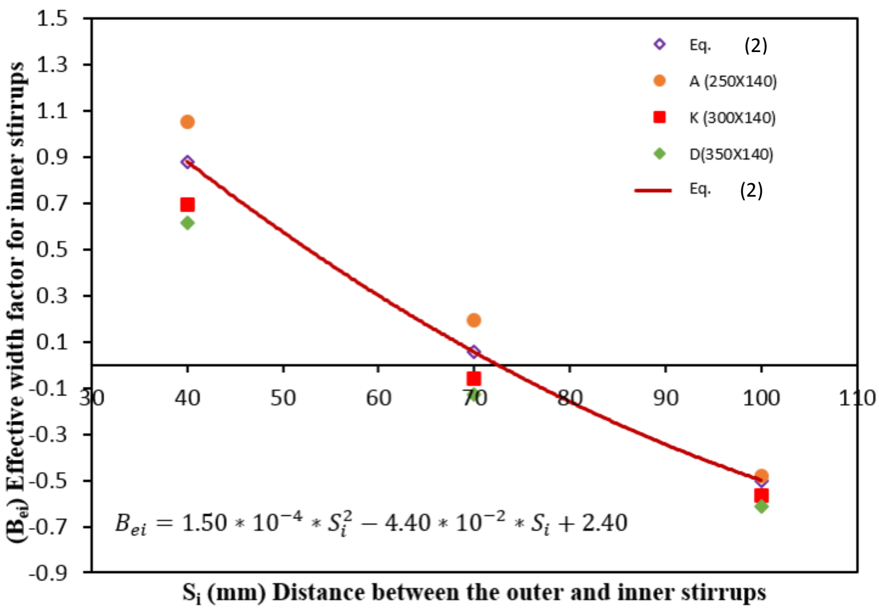

Figure (11): B_{ei} factor versus S_i distance for beams A, F and G, Other results can be found elsewhere [10]

4.2. Design guidelines

The effective width factor (B_{ei}) of inner stirrups for all tested beams was calculated according to Eq. (2), as listed in Tables 4 to 6. Moreover, Table 8 shows a comparison between the hanger failure loads with considering the (B_{ei}) calculated based on the proposed Eq. (2) and the hanger failure loads obtained from the numerical analysis of each ledge beam.

Also, table 8 shows that the hanger failure load calculated by the new proposed PCI design equation are compatible with the FEA obtained results for the most of the studied ledge beams which indicate a good agreement with the new proposed PCI design equation of the hanger steel reinforcement. It can be noticed that PCI equation overestimated the hanger capacity for ledge beams G2, G3 and G4 by 13 %.This is attributed to the overestimation of the hanger capacity of G1 and underestimated the hanger capacity for ledge beams H2, H3, H4, D2, D3 and D4 by 10% and 11% respectively. This is attributed to the underestimation of the hanger capacity of H1 and D1.

Figure 12 demonstrate a bar charts indicating the hanger load capacity for the ledge beams A1, A2, A3 and A4 with inner stirrups. The figure shows that using inner stirrups for S_i = 40 mm increase the hanger load capacity by 12.3% for S_i = 70 mm increase the hanger load capacity by 7.10 % and for S_i = 100 mm increase the hanger load capacity by 3.60 % than the ledge beam without inner stirrups, respectively.

Distribution and spacing of inner steel hanger, $A_{sh(inner)}$ reinforcement may be uniformly spaced over a width of 1.5hl on either side of the bearing.

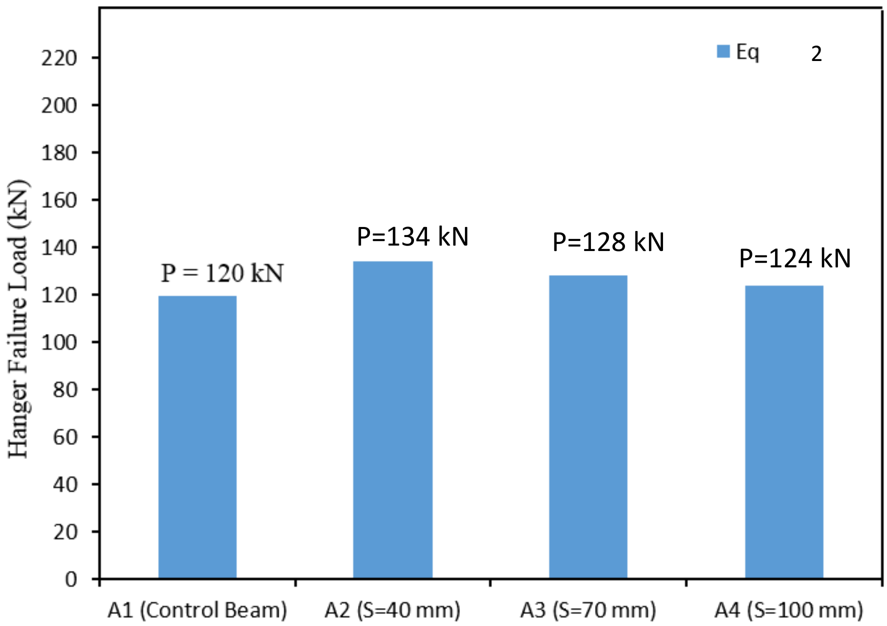

Figure (12): The hanger failure load for ledge beams A1 to A4, Other results can be found elsewhere [10]

Table (8): Comparison between both of (B_{ei}) and hanger failure load for proposed equation (2) and FEA for ledge beams.

Beam ID	Hanger capacity (kN) FEA	Hanger capacity (kN) Eq.(2)	$\frac{H\ capacity_{\ (Eq.6-2)}}{H\ capacity_{\ (FEA)}}$	B_{ei} FEA	B_{ei} Eq.2	S_i (mm)
A1	124	120	0.97	N-A	N-A	Control Beam
A2	140	134	0.96	1.05	0.88	40
A3	132	128	0.97	0.195	0.055	70
A4	127	124	0.98	-0.48	-0.50	100
K1	132	121	0.92	N-A	N-A	Control Beam
K2	146	137	0.94	0.69	0.88	40
K3	139	130	0.94	-0.06	0.055	70
K4	135	126	0.93	-0.56	-0.50	100
D1	139	124	0.89	N-A	N-A	Control Beam
D2	153	140	0.91	0.61	0.88	40
D3	146	133	0.91	-0.13	0.055	70
D4	142	129	0.91	-0.61	-0.50	100
F1	143	148	1.03	N-A	N-A	Control Beam
F2	158	165	1.04	0.65	0.88	40
F3	152	157	1.03	0.20	0.055	70
F4	147	152	1.03	-0.31	-0.50	100
M1	153	148	0.97	N-A	N-A	Control Beam
M2	172	166	0.96	1.00	0.88	40
M3	164	158	0.96	0.35	0.055	70
M4	159	152	0.96	-0.11	-0.50	100
H1	166	149	0.90	N-A	N-A	Control Beam
H2	184	168	0.91	0.84	0.88	40
H3	176	159	0.90	0.16	0.055	70
H4	170	154	0.90	-0.43	-0.50	100
G1	158	181	1.14	N-A	N-A	Control Beam
G2	178	201	1.13	0.88	0.88	40
G3	170	192	1.13	0.39	0.055	70
G4	167	185	1.11	0.31	-0.50	100
E1	173	178	1.03	N-A	N-A	Control Beam
E2	190	198	1.04	0.60	0.88	40
E3	181	188	1.04	-0.06	0.055	70
E4	177	182	1.03	-0.38	-0.50	100
J1	187	177	0.94	N-A	N-A	Control Beam
J2	214	198	0.92	1.39	0.88	40
J3	203	188	0.93	0.64	0.055	70
J4	197	181	0.92	0.21	-0.50	100

4. CONCLUSIONS

The findings of this study have shown that the inner stirrups can effectively be used as a steel hanger reinforcement to reduce the outer vertical stirrups amount. The main obtained conclusions are as follows.

1- The effective width which the hanger reinforcement transfer the vertical load acting on the ledge part in case of using outer stirrups only is (5 - 6) times the ledge beam depth each side from the acting load. This is in good agreement with The PCI Design Handbook (2010) and it deviates clearly from the values proposed in the PCA notes on ACI (318-14).

2- A general equation was developed to predict the effective width of inner stirrups hanger based on the distance between the outer and inner stirrups (Si) ,where:

a- The newly developed equation for the effective width of the inner stirrups hanger showed a good results when compared to the experimental results, where the new calculated hanger load capacity for A2, A3 and A4 showing increasing the hanger capacity by 12 %, 7 % and 3.60 %, respectively than the control beam A1 while the experimental program showing increasing the hanger capacity by 17 %, 8 % and 3 % , respectively for the same ledge beams.

b- The newly developed approach for the effective width showing that using the inner stirrups increase the hanger stirrups capacity by (11 % - 13 %) for S_i = 40 mm , (6 % -7.5 %) for S_i = 70 mm and (2.2 % - 3.8 %) for S_i = 100 mm.

c- Distribution and spacing of inner steel hanger, $A_{sh(inner)}$ reinforcement may be uniformly spaced over a width of 1.5hl on either side of the bearing.

3- The results of the proposed numerical model showed that the original PCI equation for the calculation of the hanger capacity overestimates the hanger capacity with increasing the ratios (bl/b) and (hl/h) as for G1which overestimated by 14 % where the ratio (bl/b) = 2.20 and the ratio (hl/h) = 0.43 , while it underestimates the hanger capacity with decreasing the ratios (bl/b) and (hl/h) as for H1 and D1 which underestimated by 10 % and 11% respectively where the ratio (bl/b) = 1.85 for the both and the ratio (hl/h) = 0.40 and 0.36 respectively.

5. REFERENCES

[1] ACI Committee 318 (2014). ACI 318-14: Building Code Requirements for Structural Concrete and Commentary.

[2] Mostafa, Ezz, (2015). Effect of Hanger Steel Reinforcement and Its Location on the Behavior of Ledge Beam (Phd Thesis, Faculty of Engineering, Ain Shams University).

[3] Hasan, T. (2007). Finite Element Study of Shear Behavior of Spandrel Ledges and Comparison with PCI Shear Design Provisions. Advances in Structural Engineering 10, 475–485.

[4] Hasan, T., Lucier, G., Rizkalla, S., and Zia, P. (2007). Modeling of L-shaped, precast, prestressed concrete spandrels. PCI Journal 52, 78-92.

[5] Klein, G.J. (1986a). Design of Spandrel Beams. PCI Journal 31, 76–124.

[6] Logan, D. R. (2012). "Development of a Rational Design Methodology for Precast Slender Spandrel Beams." PCI Journal 57, 182–187.

[7] Lucier, G., Walter, C., Rizkalla, S., Zia, P., and Klein, G. (2010). Development of a Rational Design Methodology for Precast Slender Spandrel Beams. North Carolina State University (Report).

[8] Lucier, G., Walter, C., Rizkalla, S., Zia, P., and Klein, G. (2011a). Development of a Rational Design Methodology for Precast Concrete Slender Spandrel Beams: Part 1, Experimental Results. PCI Journal 56, No. 2 (spring), 88–112.

[9] Precast/Prestressed Concrete Institute (2010). PCI Design Handbook 7th Edition.

[10] Badawy, Yasser" Contribution of Inner Stirrups with the Hanger Steel Reinforcement on the Behavior of Ledge Beam" PhD Thesis, Ain Shams